

# EVALUATION OF THE EROSIWE WEAR OF THE AA 6082 T6 ALLOY TREATED WITH FRICTION STIR PROCESSING

Martínez-Cámara E. <sup>(a)</sup>, Blanco-Fernández J. <sup>(b)</sup>, Chacón, Y. P. <sup>(c)</sup>, Sanchez-Roca A. <sup>(d)</sup>, Carvajal-Fals, H. <sup>(e)</sup>

<sup>(a,b)</sup> Department of Mechanical Engineering, University of La Rioja, Logroño, Spain.

<sup>(c,d,e)</sup> Faculty of Mechanical Engineering, University of Oriente, Santiago de Cuba, Cuba

<sup>(a)</sup> [ecamara@eolicas.com](mailto:ecamara@eolicas.com), <sup>(b)</sup> [julio.blanco@unirioja.es](mailto:julio.blanco@unirioja.es), <sup>(c)</sup> [yuni@fim.uo.edu.cu](mailto:yuni@fim.uo.edu.cu), <sup>(d)</sup> [sanchez@rect.uo.edu.cu](mailto:sanchez@rect.uo.edu.cu),  
<sup>(e)</sup> [carvajal@corpus.uo.edu.cu](mailto:carvajal@corpus.uo.edu.cu)

## ABSTRACT

This paper makes an evaluation of the influence of the parameters of friction stir process: number of passes and tool rotation speed, in erosive wear resistance of the alloy AA6082 T6. Samples were processed with one, two and three passes with an overlap of 100%. For the wear tests, a mixing vessel tribometer was used with rotary motion for tilt angles of particles of 30° and 90°. The number of passes, the tool rotation speed and the tilt angle of the particles has an influence on the resistance to erosive wear of the alloy AA6082T6. The best performance in terms of erosive wear resistance for the tilt angle of 30° is achieved when the material is processed at 1800 rpm with three passes. When the tilt angle of the particles was 90°, samples treated with two passes showed better erosive wear behaviour, regardless of the tool rotation speed.

Keywords: Surface, friction stir processing, wear.

## 1. INTRODUCTION

The superficial modification by Friction-Stir Processing (FSP) causes an intense plastic deformation and generates a mild heating in the processed area; these thermodynamic conditions favour the development of recrystallized fine grains, with excellent properties, resistance to fatigue, corrosion and superficial wear. This process is considered to be the most relevant in terms of metal welding over the last two decades. It is widely used in automotive and aeronautics applications with remarkable results (Uday 2010; Aldanondo 2011). Many researches have been devoted to FSW of aluminium alloys (Hassan 2010; Szkodo 2010; Xunhong 2008; Cavaliere 2008, Fernandez et al, 2012; Orozco et al, 2012, 2013; Jimenez et al, 2010, 2014).

Santella (2005) studied the effect of the application of FSP over the mechanical properties of molten aluminium alloys (A356 and A319) and observed a fine equiaxial microstructure in the stir zone; the tensile strength, ductility and resistance to fatigue of both alloys improved.

The application of FSP with multiple passes for the creation of superplastic 7075 aluminium was studied by Johannes and Mishra (2007).

Magdy (2012) reported an increase of the hardness with the increase of processing speed, which decreases with the increase of the number of passes in the

aluminium alloy AA 6082-T9. They also concluded that with the increase of the number of passes the tensile strength increases.

Most researches study the influence of the application of the FSP in the microstructure, micro-hardness and tensile strength (Martinez-de-Pison et al, 2010, 2012); and there is a lack of studies about the influence of the FSP parameters in the resistance to wear. This paper assesses the influence of the parameters: number of passes and tool rotation speed in the erosive wear of the aluminium alloy AA 6082-T6 modified by the FSP technique.

## 2. MATERIALS AND METHODOS

The material used for this research was the aluminium alloy AA 6082-T6. The chemical composition (wt%) of the material used for this research was as follows Si = 1,2; Fe = 0,5; Mn = 0,95; Mg = 1; Cu = 0,10; Cr = 0,25; Zn = 0,20; Al = 95,65 and 0,15 corresponding to other elements. The dimensions of the test samples were 150x150x3 mm.

The FSP process was made by means of a CNC milling machine with position control and three tool rotation speeds were used (710, 1120 and 1800 rpm) and a constant tool advancing speed of (100mm/min), with a variation from 1 to 3 passes and a 100% overlapping for each pass.

The processing of the material was made perpendicular to the laminating direction. The inter-pass temperature was constant and room temperature was always used.

The tool used was made of AISI D2 steel, and was designed with a fluted cylindrical probe, 3mm diameter and 1.6 mm long. The tool shoulder has a diameter of 10mm with a concave profile.

Measuring of the micro-hardness was made in the different regions of the transversal section of the material treated. The measuring was made using a micro-hardness tester "Shimadzu Micro Hardness Tester Type M". The weight used to measure micro-hardness was of 25 grams with duration of five seconds.

The tests of erosive wear were made with a tribometer of mixture recipient with rotatory motion and two devices were used with a tilt angle of 30° and 90°. The area exposed to erosive wear was removed from the processed zone, without any influence of the base metal.

Figure 1 shows a representative image of the FSP process and erosion test.

The erosive mixture was composed of distilled water (1.8 litres) and abrasive particles of silica sand (300 g/litre). The size of the abrasive particles ranged from 30 and 50  $\mu\text{m}$  diameter (Figure 2) (Roca et al., 2007, 2008, 2009). An on-line monitoring system was implemented to detect the changes of the tool profile reflected in the vibroacoustic signal (Figure 1).

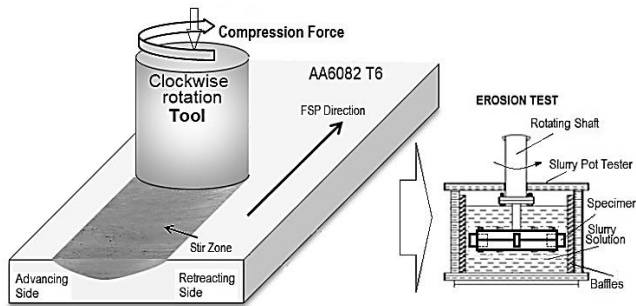


Figure 1. Representation of Friction Stir Process and Slurry Pot Tester

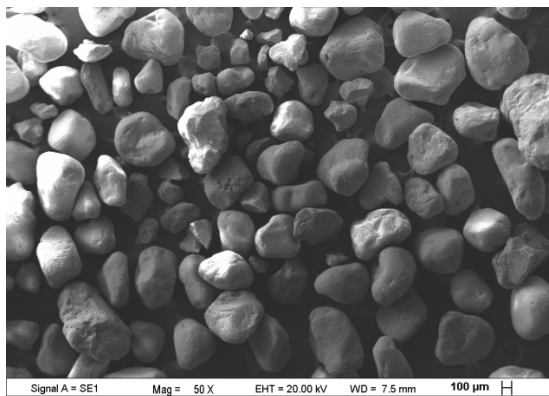


Figure 2: Silica abrasive particles

The impact speed of the particles was of 4.15 m/s and the tests were made for 3 hours, with 30 minute intervals. The wear was determined by the difference in weight of the samples before and after each pass; the erosive mixture was substituted by each interval and all the tests were repeated 3 times.

### 3. RESULTS AND DISCUSSION

Figure 3 shows the different areas in the process zone, such as, nugget zone (NZ), thermo mechanically affected zone (TMAZ), and heat affected zone (HAZ). In Figure 3, one can observe the good quality of the regions. The macro-images of the process zone presented in Fig. 3 show no defects and macro-structural continuity.

The tool rotation speed and the number of passes influenced the microstructural transformations that took place in the surface of the material. In the nugget zone,

a total recrystallization of the grains took place and in the thermo-mechanically affected zone, a partial recovery.

An image corresponding to the experimental condition of 710 rpm with one pass, representative macrostructure is shown in Figure 3. Figure 1 shows the vibro-acoustic signals corresponding to two conditions with the same process parameters ( $\omega = 450 \text{ rpm}$ ,  $v = 100 \text{ mm}\cdot\text{min}^{-1}$ ) and for the two different tool profiles evaluated.

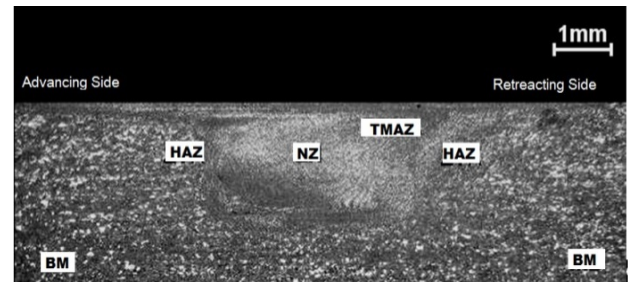


Figure 3. Representative macrograph image of the cross section of specimens processed with 710 rpm and one pass.

A central zone or core can be seen, which corresponds to the material that is subjected to stirring in plastic state where a high refining of the size of the grain occurs. Later on, a thermo-mechanically affected zone where the material suffers a high deformation and the elongated grains of the base metal are deformed in an advancing flow pattern around the core. Following that, a thermo-mechanically affected zone can be seen at both sides of the footprint left by the tool, characterized by the occurrence of a thermal cycle where the grains keep the same structure of the base metal and finally the area of the base metal where one can see the microstructure of the original material.

In both zones, the fine precipitates ( $\beta\text{-Mg}_5\text{Si}_6$ ), present in the base metal and responsible for the hardening of the original material, were dissolved in the matrix and did not re-precipitate when using 710 rpm and 1200 rpm.

A precipitate of a bigger size was formed in the thermo-mechanically affected zone ( $\beta\text{-Mg}_1.7\text{Si}$ ), corroborating the results of Moreira (2009). The processes of recrystallization, microstructural recovery and solubilisation (710 rpm y 1200 rpm), and the reformation of new precipitates (1800 rpm) caused changes in the strength of the material and thus influenced the behaviour of the erosive wear of the aluminium alloy AA 6082-T6.

Figure 4 shows a representation of the micro-hardness profile of the cross section of one of the samples for the condition with 710 rpm and three passes.

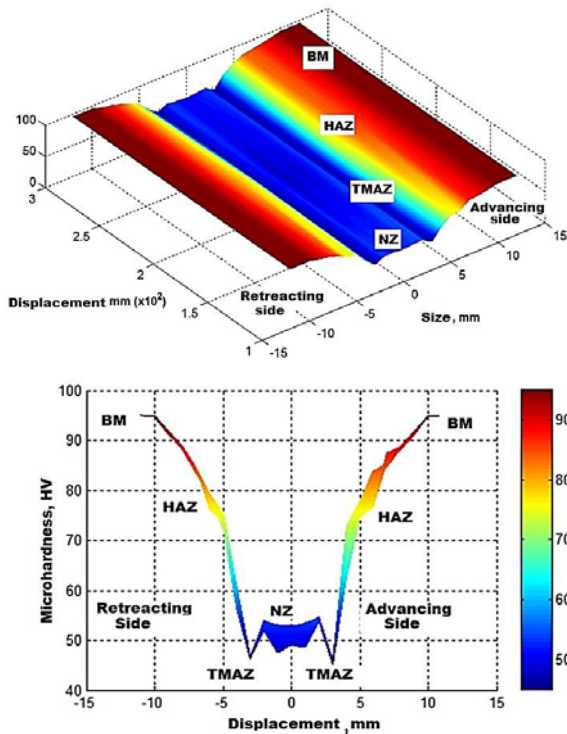


Figure 4: Micro-hardness behaviour for 710 rpm and three passes. UP) Aerial view; DOWN) Cross section.

The core zone (ZN) experiences a decrease in micro-hardness due to the deformation of the material and the changes resulting from the dynamic recrystallization that takes place in the process. It can also be seen that in the thermo-mechanically affected zone (ZTMA), there is a minimum of micro-hardness compared to the ZN more inclined to the advancing side of the tool.

According to Sterling (2005), the distribution of the micro-hardness profiles is due to the different morphologies, grain sizes and the bands of deformed material. These authors assert that, the microstructural result is due to the processes of dynamic restoration-recrystallization reached, in accordance with the thermal cycle and the variation of the deformation speed. The latter decreases rapidly as the tool pin separates due to the viscous dissipation of the plastically deformed material in the core and the ZTMA, both in a horizontal and vertical way (Nandan, 2008).

Figure 5 shows the micro-hardness maps in accordance with the number of passes for the tool rotation speed of 710rpm.

Figure 5 shows that for the condition 710 rpm the higher values of micro-hardness are reached when the material is processed with one pass, which is attributed to the refining of the size of the grain of the superficial layer of the process of dynamic recrystallization that takes place in the zone. This corroborates the results of Surekha (2009), Mishra (2005) and Mroczka and Pietras (2009) who assert that, with a lower heat input, that is, a low rotation speed, a structure with a quite refined grain is obtained.

On the other hand, with the increase of the number of passes at the same tool rotation speed, the micro-hardness decreases due to the growth of the grain of the superficial layer resulting from the thermal cycles accumulated in each pass, parallel to the continuous dynamic recrystallization that takes place. This result ratifies what Johannes and Mishra (2007) have stated in previous works.

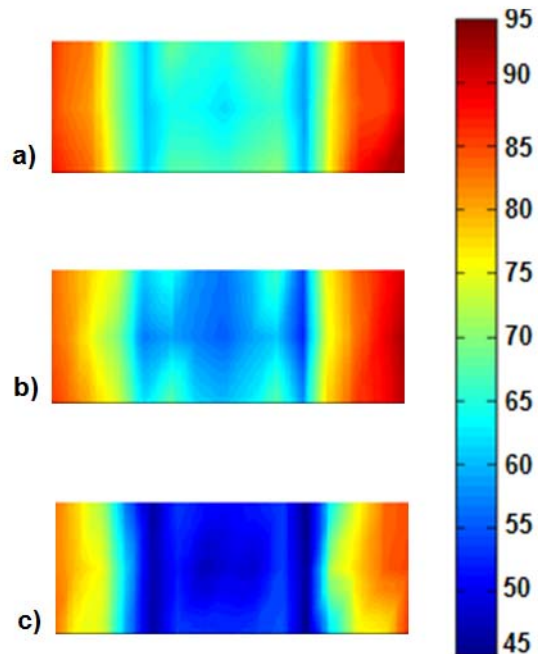


Figure 5: Micro-hardness maps for 710 rpm of tool rotation speed. a) 1 pass, b) 2 passes, c) 3 passes.

Figure 6 shows the results of the accumulated erosive wear for the different combinations of parameters and tilt angle of the particles of 30°.

The curves obtained (Figure 6) show that the increase in tool rotation speed and number of passes are influential factors in the increase of resistance to wear. In general, it can be asserted that the best behaviour for the 30° tilt angle takes place when the material is processed with three passes at 1800 rpm.

Likewise, Figure 7 shows a graph with the results of the accumulated erosive wear, in the form of accumulative mass loss, for the different combinations of parameters and tilt angle of the particles of 90°.

In the curves shown in Figure 7, it can be seen that the increase in tool rotation speed diminishes the resistance to erosive wear. When the tilt angle of the particles was 90°, the samples with the best behaviour to erosive wear were those processed with two passes, regardless of the tool rotation speed; and when three passes are made, the resistance to erosive wear diminishes. The best behaviour for the tilt angle of 90° takes place when the material is processed with two passes at 710 rpm of tool rotation speed.

It was thus proved that the tilt angle of the particles influences significantly the loss of weight, which is related to the change in the wear mechanism (Wang, 2008). It could be seen that the loss of weight by

erosive wear with tilt angle of the particles of 30° was higher in the samples processed at 710 rpm with two passes as well as the samples processed at 1200 rpm with two and three passes.

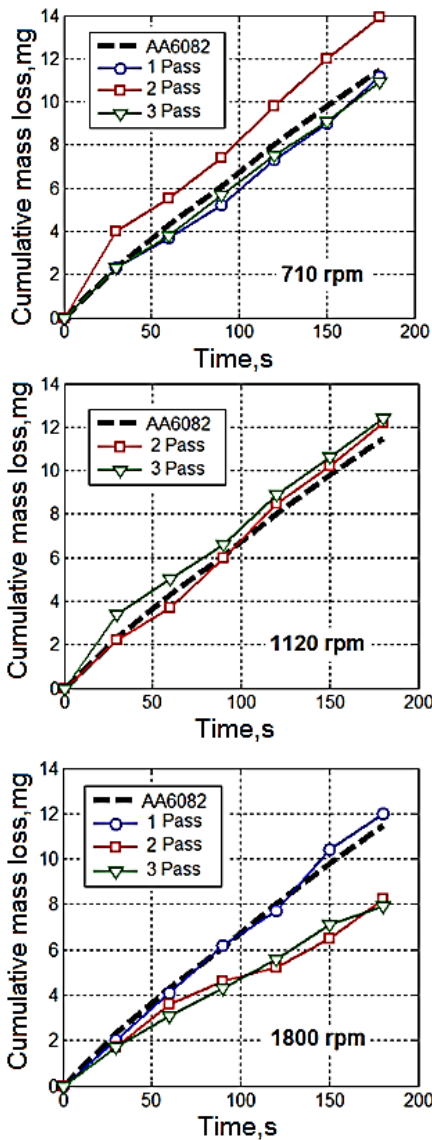


Figure 6: Graph of the loss of weight accumulated in the erosive wear for a tilt angle of the particles of 30°.

Under such processing conditions, a loss of superficial hardness occurred because of the solubilisation of the precipitates responsible for the hardening of the material.

This behaviour corroborates the results obtained by Magne (1991). This author explains that the materials with lower hardness have lower resistance to erosive wear when the tilt angle of the particles is small, with a predominance of the wear by micro-cuts (figure 8). Figure 8 and 9 shows a micrograph of the worn surface where this kind erosive wear mechanism can be seen.

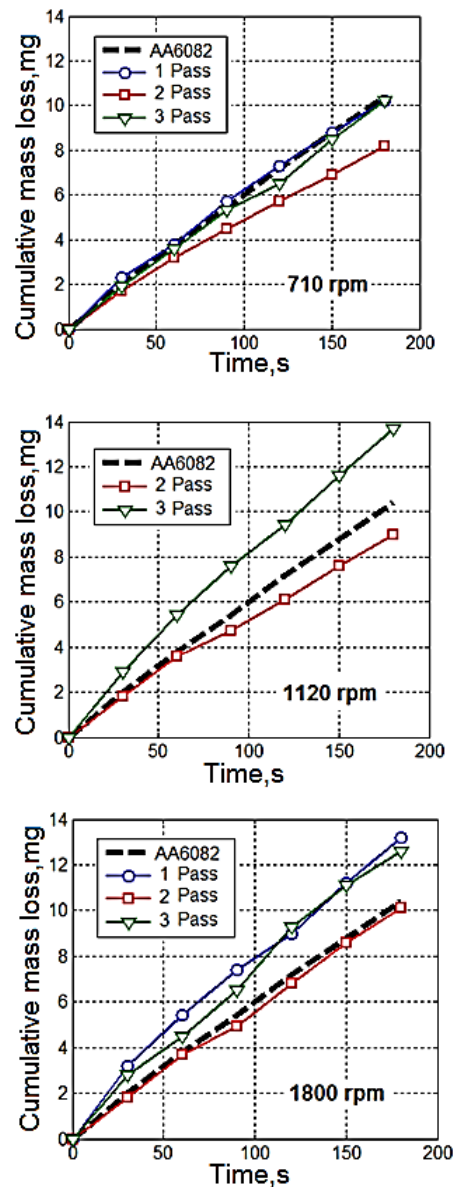


Figure 7: Graph of the loss of weight accumulated in the erosive wear for a tilt angle of the particles of 90°.

For the test samples processed at 1800 rpm, it was proved that the higher value of erosive wear takes place when the tilt angle of the particles is of 90°.

When the process uses 1800 rpm tool rotation speed, there is a change in the properties of the material, increasing the superficial hardness as a result of the formation of new precipitates in the processed zone. The process temperature increase and a lower cooling temperature, when 1800 rpm were used, causes the formation of new fine precipitates, probably type  $\square$ Mg<sub>5</sub>Si<sub>6</sub>, which constitute obstacles to the process of deformation of the material, and lead to the hardening of the stir zone by precipitation.

The superficial processing of the material at 1800 rpm, caused a change in the mechanism of erosive wear, taking place mainly a wear by deformation with extruded edges (Figure 9).

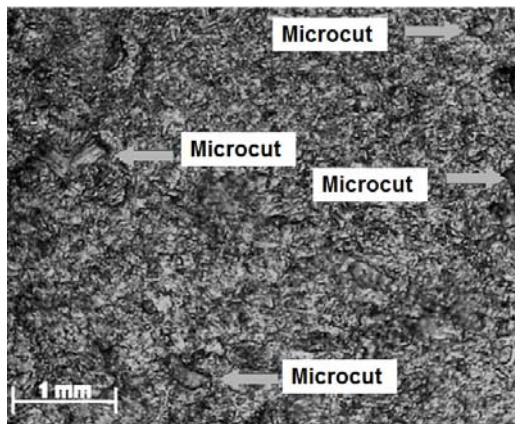


Figure 8. Micrograph of the erosive wear surface for a tilt angle of the particles of  $30^{\circ}$  and the condition of 710 rpm and 3 passes.

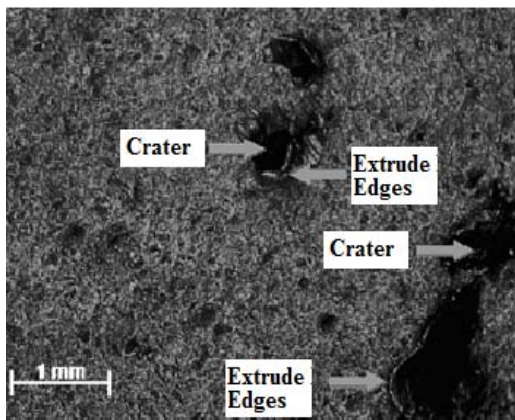


Figure 9: Micrograph of the erosive wear surface for a tilt angle of the particles of  $30^{\circ}$  and the condition of 710 rpm and 3 passes.

It is thus evident that the wear mechanism corresponds to the findings published in the literature consulted (Magne 1991), and is related to the way of eliminating the wear surface; in these cases, the wear comes as a result of the successive impact of particles that are normally projected and cause primarily the impregnation in the surface of the material. It is possible that in these cases the plastic and elastic deformations of the worn surfaces coincide. This means that extruded edges are formed from plastically deformed zones that come in the form of wear particles.

Finally, it can be said that, the number of passes with a 100% overlapping, the tool rotation speed and the tilt angle of the particles, influence the resistance to erosive wear of the aluminium alloy AA 6082 T-6, treated with friction stir processing.

It can also be concluded that when the tilt angle of the particles is of  $30^{\circ}$ , the increase of the tool rotation speed and the number of passes cause an increase in the resistance to erosive wear of the aluminium alloy AA 6082 T-6. Furthermore, with a  $90^{\circ}$  tilt angle of the particles, the increase of the number of passes at a tool

rotation speed of 710 rpm caused an increase in the resistance to erosive wear of the samples analysed.

#### 4. CONCLUSIONS

This research paper shows the influence of the parameters, number of passes and tool rotation speed, in the resistance to erosive wear of the aluminium alloy 6082-T6 modified by the FSP process. From the analyses conducted, it can be concluded that:

1. The number of passes with a 100% overlapping, the tool rotation speed and the tilt angle of the particles influence the resistance to erosive wear of the aluminium alloy 6082-T6 treated with the Friction Stir Process.
2. When the tilt angle of the particles is  $30^{\circ}$ , the increase in tool rotation speed and number of passes cause an increase in the resistance to erosive wear of the aluminium alloy 6082-T6.
3. The best behaviour for the tilt angle of  $30^{\circ}$  occurs when the material is processed with two and three passes at a tool rotation speed of 1800 rpm.
4. For a tilt angle of the particles of  $90^{\circ}$ , the increase in the number of passes at a tool rotation speed of 710 rpm caused an increase in the resistance to erosive wear in the analysed samples.
5. The best behaviour for the tilt angle  $90^{\circ}$  occurs when the material is processed with three passes at a tool rotation speed of 710 rpm.

#### ACKNOWLEDGMENTS

This paper has been partially supported by the project of the Ministry and Innovation "DPI2011-25007. Soldadura por fricción-agitación de materiales disimilares. Caracterización mediante técnicas de emisión acústica e inteligencia artificial".

#### REFERENCES

- Aldanondo, E., 2011. Avances en la tecnología de soldadura por fricción "STIR". DYNA Ingeniería e Industria. 86(6): 614-618.
- Cavaliere, P., Panella, F., 2008. Effect of tool position on the fatigue properties of dissimilar 2024-7075 sheets joined by friction stir welding. J. of Mater. Proc. Technol., 206: 249-255.
- Fernández, J.B., Roca, A.S., Fals, H.C., Macías, E.J., de la Parte, M.P. 2012. Application of vibroacoustic signals to evaluate tools profile changes in friction stir welding on AA 1050 H24 alloy. Science and Technology of Welding and Joining 17(6):501-510.
- Hassan, A.S. 2010. Friction stir welding of dissimilar A319 and A356 aluminium cast alloys. Sci. Technol. Weld. Join. 15(5): 414-422.
- Jiménez-Macías, E., Sánchez-Roca, A., Carvajal-Fals, H., Blanco-Fernández, J., Martínez-Cámara, E. 2014. Wavelets application in prediction of

- friction stir welding parameters of alloy joints from vibroacoustic ANN-based model. *Abstract and Applied Analysis*. Volume 2014, Article number 728564.
- Johannes, L.B., Mishra, R.S., 2007. Multiple passes of friction stir processing for the creation of superplastic 7075 aluminium. *Materials Science Engineering A*, 464: 255 – 260.
- Magdy, M., Ehab, A., 2012. The influence of multi-pass friction stir processing on the microstructural and mechanical properties of aluminium alloy 6082. *Journal of Materials Processing Technology*, 212: 1157 – 1168.
- Magne A., *Etude des processus d'usure de matériaux métalliques soumis à l'abrasion et à l'érosion*. Thesis, University of Liege.
- Mishra R.S., Ma, Z.Y., 2005. Friction stir welding and processing. *Material Science and Engineering R*, 50: 1- 78.
- Moreira, P.M., et al. 2009. Mechanical and metallurgical characterization of friction stir welding joints of AA6061-T6 with AA6082-T6. *Materials and Design*, 30: 180–187.
- Mroczka K., Pietras A., 2009. FSW characterization of 6082 aluminum alloys sheets. *Archives of Materials Science and Engineering*, 40(2): 104 - 109.
- Nandan R. et al., 2008. Recent advances in friction-stir welding – Process, weldment structure and properties. *Progress in Materials Science*, 53 (6) : 980–1023,
- Orozco, M.S., Macías, E.J., Roca, A.S., Fals, H.C., Fernández, J.B. 2012. Optimisation of friction-stir welding process using vibro-acoustic signal analysis. *Science and Technology of Welding and Joining* 18 (6): 532-540
- Santella M.L., Storjohann E., Pan, T.Y., 2005. *Scripta Material* 53:201.
- Su J., Nelson T., Sterling C., 2005. Microstructure evolution during FSW/FSP of high strength aluminum alloys. *Materials science and engineering, A*, 405: 277–286,
- Szkodo, M., Adamowski, J., Sitko, A., 2010. Assessment of FSW Welds Made of Aluminum Alloy AW7075-T651. *Solid State Phenom.*165: 201-206.
- Surekha, B. Murty, K., 2009. Effect of processing parameters on the corrosion behaviour of friction stir processed AA 2219 aluminium alloy. *Solid State Sciences* 1: 907–917.
- Uday, M.B., 2010. Advances in friction welding process: a review. *Sci. Technol. Weld. Join.* 15(7): 534-558.
- Wang Y, Yang Z (2008) Finite element model of erosive wear on ductile and brittle materials *Wear* 265: 871 – 878.
- Xunhong, W., 2008. Comparison of fatigue property between friction stir and TIG welds. *Journal Univ. Sci. Technol. Beijing.*15(3): 280-284.
- Cesar Sanchez-Orozco, M., Blanco-Fernandez, J., Jimenez-Macias, E., & Perez-delaParte, M. (2013). VIBROACOUSTICAL SIGNALS TO EVALUATE TOOL PROFILES ON FRICTION STIR WELDING PROCESS. *Dyna*, 88, 318-324. doi: 10.6036/5326
- Javier Martinez-de-Pison, F., Sanz, A., Martinez-de-Pison, E., Jimenez, E., & Conti, D. (2012). Mining association rules from time series to explain failures in a hot-dip galvanizing steel line. *Computers & Industrial Engineering*, 63, 22-36. doi: 10.1016/j.cie.2012.01.013
- Jimenez Macias, E., Sanchez Roca, A., Carvajal Fals, H., Blanco Fernandez, J., & Perez de la Parte, M. (2010). Time-frequency diagram applied to stability analysis in gas metal arc welding based on acoustic emission. *Science and Technology of Welding and Joining*, 15, 226-232. doi: 10.1179/136217109x12665778348588
- Martinez-de-Pison, F. J., Pernia, A., Jimenez-Macias, E., & Fernandez, R. (2010). Overall model of the dynamic behaviour of the steel strip in an annealing heating furnace on a hot-dip galvanizing line. *Revista De Metalurgia*, 46, 405-420. doi: 10.3989/revmetalm.0948
- Roca, A. S., Fals, H. C., Fernandez, J. B., Macias, E. J., & Adan, F. S. (2007). New stability index for short circuit transfer mode in GMAW process using acoustic emission signals. *Science and Technology of Welding and Joining*, 12, 460-466. doi: 10.1179/174329307x213882
- Sanchez Roca, A., Carvajal Fals, H., Blanco Fernandez, J., Sanz Adan, F., & Jimenez Macias, E. (2008). Stability analysis of the gas metal arc welding process based on acoustic emission technique. *Soldagem & Inspecao*, 13, 61-69.
- Sanchez Roca, A., Fals, H. C., Fernandez, J. B., Macias, E. J., & de la Parte, M. P. (2009). Artificial neural networks and acoustic emission applied to stability analysis in gas metal arc welding. *Science and Technology of Welding and Joining*, 14, 117-124. doi: 10.1179/136217108x382981